The atmosphere structure and meteorology instrument on the Mars Pathfinder lander

Alvin Seiff,[1,2] James E. Tillman,[3] James R. Murphy,[1,2] John T. Schofield,[4] David Crisp,[4] Jeffrey R. Barnes,[5] Clayton LaBaw,[4] Colin Mahoney,[4] John D. Mihalov,[6] Gregory R. Wilson,[2,7] and Robert Haberle[6]

Abstract.   An instrument on the Pathfinder lander has been designed to measure the structure of Mars' atmosphere during spacecraft entry and descent from ~150 km altitude to the surface, and to measure meteorological parameters after landing for the landed duration of the mission. This is specified to be nominally 30 Mars days but potentially up to 1 Earth year. Landed sensors will measure surface level pressure; temperatures at 0.25, 0.5, and 1.0 m above the surface; and wind speed and direction at a height of 1.1 m. These sensors are mounted on a slender mast about 1.63 m from the center of the Lander base petal so as to avoid flow disturbance and thermal contamination insofar as possible. Wind sensing is most sensitive at velocities <20 m s^{-1} but can resolve speeds up to 50 m s^{-1}, with directional accuracy ~10°. A key point of interest in atmosphere structure is comparison with profiles obtained by Viking 20 years ago, to evaluate changes predicted to occur with solar activity and with dust loading of the atmosphere. The proximity of the landing site to that of Viking Lander 1 will permit comparison with and extension of the earlier lander data, which were taken over a period of more than 3 Mars years. The improved sensitivity of the lander instruments will also permit investigation of many new phenomena.

Introduction

The existing in situ data on the atmosphere of Mars were largely acquired by atmosphere structure and meteorology instruments on the two Viking landers. Together, the atmosphere structure sensors and the upper atmosphere mass spectrometer measured the atmosphere from an altitude of 200 km essentially to the surface during entry and descent [*Seiff and Kirk*, 1977; *Nier and MacElroy*, 1977]. On the surface the meteorology experiment measured winds and temperatures at a height of 1.6 m and pressures near the surface for over 3 Mars years [*Hess et al.*, 1977; *Tillman et al.*, 1993; *Leovy et al.*, 1985].

Viking was enormously successful in advancing our knowledge and understanding of the atmosphere of Mars, but it was limited to 2 sites over ~3 Mars years. It measured temperature and wind at only one elevation and was limited to 10-bit resolution. Wind measurements were also acquired, however, during parachute descent [*Seiff*, 1993]. The Pathfinder lander presents the first opportunity since Viking for in situ measurements in Mars' atmosphere. It will respond to all of the above limitations by exploring conditions (1) at a third site, although one close in latitude to Viking 1; (2) in another Mars year; and (3) at 14-bit

resolution, which should enable the detection of smaller perturbations than those which could be reported by the Viking sensors.

The Pathfinder atmospheric structure and meteorology instrument (ASI/MET) investigations will be carried out both during entry and descent and after landing. During high-speed entry, atmospheric densities will be measured using accelerometers. This mission phase ends at parachute deployment, nominally at 8 km altitude. During parachute descent, pressure and temperature will be measured by sensors sampling the atmosphere just inside one of the lander window openings. On the surface the lander petals will be opened to set the lander upright (Figure 1), and a meteorology mast will be deployed. This mast is a slender wand, 1 cm in diameter × 1.1 m high. It is located at the tip of one of the solar panels to place it as far as possible (~1.63 m) from the lander center, where the electronics box is a heat source to be avoided. The mast carries temperature sensors at three heights and a wind sensor on its top. Three "wind socks" are also mounted on the mast at heights intermediate between the temperature sensors. Surface pressure will be measured after landing, through the same inlet and by the same sensor used in parachute descent. The inlet is just ~10 cm above the planet surface.

The pressure sensor is a Tavis variable reluctance, deflecting diaphragm unit, of the same type used successfully on Viking. The temperature sensors are chromel-constantan thermocouples, triply redundant within each sensor. The wind sensor is a new design, basically multiple hot wire anemometers with directional and magnitude capability. The accelerometers are sensitive servo accelerometers of the type used for aircraft inertial guidance, located near the center of gravity of the lander during entry.

The meteorology experiment is required to operate on the surface for a minimum of 30 Mars days (sols), and should be capable of operating for an Earth year (a design goal). In the following sections, we first describe science objectives and then key aspects of the ASI/MET instrument for each of its functions,

---

[1]San Jose State University Foundation, San Jose, California.
[2]Now at Ames Research Center, Moffett Field, California.
[3]Atmospheric Science Department, University of Washington, Seattle.
[4]Jet Propulsion Laboratory, NASA, Pasadena, California.
[5]Atmospheric Sciences Department, Oregon State University, Eugene.
[6]Space Science Division, Ames Research Center, NASA, Moffett Field, California.
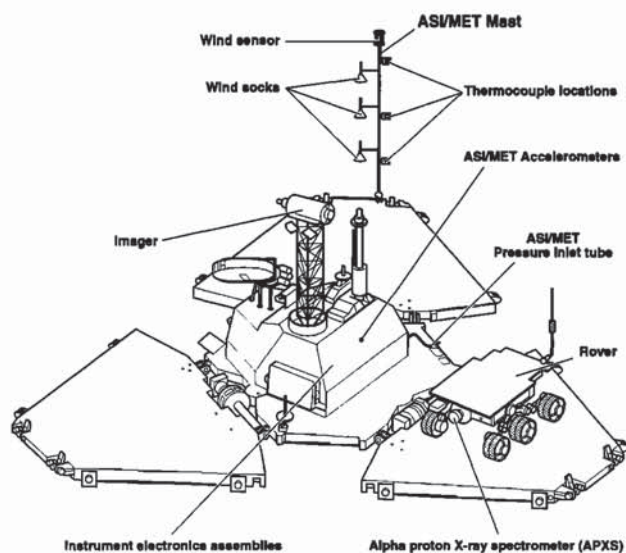[7]Geology Department, Arizona State University, Tempe.

Figure 1. The Pathfinder lander as it will be deployed after landing on Mars and opening its three solar panels. At the tip of the far panel the meteorology mast is shown erected, with three sets of temperature sensors in position to measure the temperature profile in the near-surface boundary layer, and the three wind socks deployed. The wind sensor sits atop the mast.

first the entry and descent phase structure measurements, and then the longer term landed phase meteorology measurements.

Science Objectives

The general scientific objectives in the study of planetary atmospheres are (1) to determine the three-dimensional structure of an atmosphere (composition, pressure, density, temperature, aerosols, winds) and its variation in time, (2) to understand the response (the "general circulation") of an atmosphere to its "external" forcing (solar heating), and (3) to understand the origin and subsequent evolution of an atmosphere. Key measurements for objective 1 are the composition, pressure, density, temperature, wind, and aerosols in the atmosphere as functions of time. For objective 2, the forcing (solar heating of the surface and atmosphere) needs to be measured/calculated and related to the observations of objective 1 using theory and models. For objective 3, measurements that bear upon the origin and evolution of the atmosphere need to be made (e.g., rare gas abundances and isotopic ratios) and paleoclimatic indicators (e.g., ice cores) need to be identified and analyzed; finally, theories and models must be constructed and tested.

A surface lander equipped to make meteorological measurements in situ in the atmosphere of Mars can address the above objectives in several ways. The Pathfinder ASI/MET experiment, in particular, will obtain measurements to determine pressure, density, and temperature as functions of height from about 150 km down to the surface in the atmosphere above the landing site at the time of entry, descent, and landing. Once on the surface, the MET instruments will obtain measurements of pressure, temperature, and winds (speed and direction), while the Pathfinder imager (IMP) will obtain intermittent measurements of aerosols [*Smith et al.*, this issue]. The temperature measurements will be made at three different heights (about 0.25, 0.5, and 1.0 m), and wind measurements will be obtained at a

height of 1.1 m. The pressure measurements will be made essentially at the surface elevation of the landing site. All of these quantities will be sampled at least once every hour (there being multiple measurements in every sample) to provide excellent coverage of their diurnal variations at the landing site. The repeating coverage from day to day will allow the variations of these basic atmospheric variables to be monitored on longer timescales, hopefully, as long as a year or more.

The two Viking landers made similar meteorological measurements on Mars from 1976 to 1982. The Pathfinder landing location is relatively close to the Viking Lander 1 site, which has an advantage of facilitating comparison of the data with the previous Viking data. (This landing site was, however, selected primarily based on spacecraft landing safety and geological considerations [*Golombek et al.*, this issue].) On the other hand, the Pathfinder site will not extend to regions of the planet that have not been sampled (e.g., the southern hemisphere and the polar regions).

Mars atmospheric pressure measurements are both operationally and scientifically valuable. Scientifically, even surface-based measurements provide insights into a wide range of atmospheric phenomena. Although local, regional, synoptic, and global phenomena can contribute to the same signal, these phenomena can often be distinguished from each other and quantitatively studied. Previous studies have treated synoptic processes, atmospheric tides, global oscillations, the determination of optical depth, and the annual variation due to polar cap condensation and sublimation, and the interannual similarity during nominally dust free years [*Barnes*, 1981; *Hess et al.*, 1977, 1979, 1980; *James and North*, 1982; *Leovy and Zurek*, 1979; *Leovy*, 1981; *Leovy et al.*, 1985; *Paige and Wood*, 1992; *Ryan et al., 1978*; *Ryan and Henry*, 1979; *Tillman*, 1977, 1985, 1988; *Tillman et al.*, 1979, 1993; *Wood and Paige*, 1992; *Zurek*, 1981, 1988; *Zurek et al.*, 1992].

The nominal landing date, July 4, 1997, at $L_s = 142°$, is near the annual pressure minimum corresponding to maximum condensation in the southern polar region (Figure 2). Since Pathfinder's latitude, 19.5°N and longitude, 32.8°, are close to those of Viking Lander 1, 22°N, 48°, the latitudinally dependent meteorological processes should be very similar to those of Viking 1, for which observations in this season are available in 4 Mars years. Comparison with Pathfinder data will indicate which, if any, Viking year they resemble. If local topographic differences have a strong effect on the local meteorology, the comparison could be invalidated, but it would still be informative.

Pathfinder's goal of 1 year of operation on the surface would permit comparisons with the "nominal, low dust" annual pressure cycle established by *Tillman et al.* [1993], when adjusted for mean pressure differences. It would also mark the fifth year of observations around solar longitude 210°, the beginning of the great dust storm season. Two of the four Viking years showed "great dust storm" activity, so it would not be unexpected to observe such a storm, although it appears that the Viking years were exceptionally dusty years.

An objective of the early mission pressure measurements will be to search for transient pressure perturbations, hypothesized to be transient Kelvin waves [*Tillman*, 1988]. These can be observed during the seasonal range $130° < L_s < 157°$ (solar longitude), which is the season of Pathfinder landing. Their observation earlier or later near summer solstice was precluded by the Viking pressure resolution of 0.088 mbar.

Viking lander 2 pressure did not vary by one digital number (DN) on some sols. With the roughly 100X higher resolution of
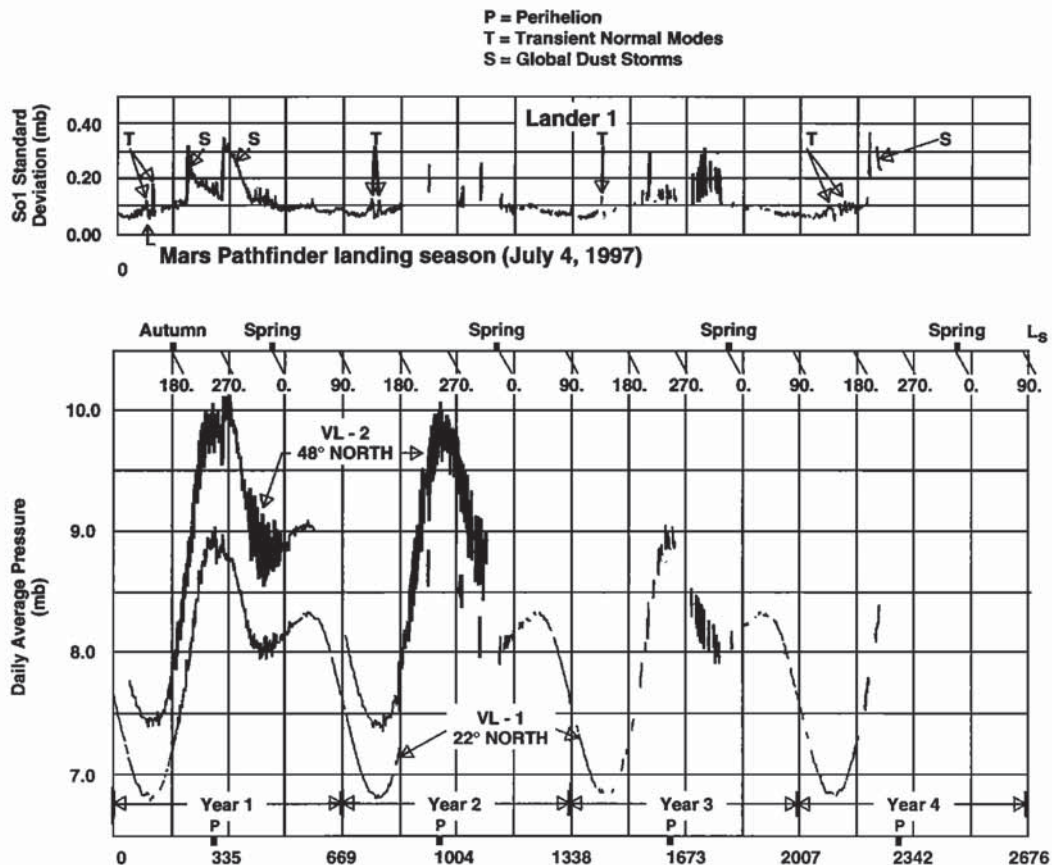
Figure 2. The Mars Pathfinder landing date in late spring is indicated in the context of the Viking pressure data collected by the two landers over 3.36 Mars years. The bottom plot shows the daily mean pressures, while the upper plot shows the standard deviations about the mean. Note the transient normal modes, labeled T, occur around $L_s = 145°$, just after the Pathfinder landing, and the great dust storms, labeled S, begin near $L_s = 210°$ and $L_s = 270°$ [*Zurek et al.*, 1992].

the Pathfinder system, it will be possible to scan data over a longer time and wider range of atmospheric pressures than was possible from Viking and establish wave frequency and amplitudes. The spectral characteristics of the diurnal and Kelvin harmonics vary from year to year and also may help decide which Viking year the early Pathfinder observations most closely resemble, or that it clearly differs from all observed years. Theory for such Kelvin waves [*Zurek*, 1988] gives the frequency and amplitude as functions of atmospheric parameters and will provide a foundation for the evaluation of the Kelvin mode hypothesis.

Like Earth, Mars has lower synoptic activity during late spring and early summer. The higher resolution will allow better characterization or specify limits for this activity during summer. Significant baroclinic activity occasionally penetrated as far south as the Viking 1 site, especially during winter years without great dust storms. Similar activity would be expected at the Pathfinder site if global conditions are similar to the very active years, such as the one during which artificially created soil piles were eroded [*Arvidson et al.*, 1983].

The Viking landers obtained the only existing in situ measurements of atmospheric temperatures near the surface of Mars. Each lander measured atmospheric temperatures from a single boom-mounted thermocouple sensor that was located at a height of 1.6 m above the Martian surface. Measurements collected by these sensors during the 3.4 Mars year lifetime of the Viking landers revealed large diurnal (40 to 60 K) and seasonal (60 to 80 K) temperature variations, as well as significant (1 to 3 K) temperature changes on timescales as short as 10 s. These measurements have been widely used for studies of the thermal balance of the surface and near-surface atmosphere of Mars, diurnal variations in the depth of the planetary boundary layer, and the effects of these processes on the Martian general circulation. They have also provided important environmental constraints on the design of subsequent Mars landers.

The Mars Pathfinder lander provides the first opportunity to obtain near-surface temperature measurements from another site on Mars. It also provides the first opportunity to obtain simultaneous measurements from more than one level, to resolve vertical gradients in the near-surface temperatures. This should enable much to be learned about the structure of temperature in the surface layer of the atmosphere. In particular, it should be possible to infer (using theory and models) the transfer of heat from the surface to the atmosphere at the landing site. This is a crucial quantity for objective 2 above. Together with the wind measurements, the temperature measurements should allow at least estimates of the surface stress to be made as well. This quantity is also critical to objective 2. Other instruments on Pathfinder will

aid in addressing objective 2 also, in particular the camera (IMP). It will provide observations of atmospheric aerosols and dust, their particle size, refractive index, and altitude distribution. These influence the radiation field and affect atmospheric temperatures, and thus play an important role in atmospheric dynamics. IMP will also provide measurements of the total amount of water vapor in the atmosphere at the landing site, and the relation of this to the MET temperature data should enable a better understanding of the behavior of atmospheric water on Mars. This is relevant to the evolution of the Mars atmosphere and climate system, as well as to its present state.

Pathfinder ASI measurements made while the lander traverses the upper and middle atmosphere will be relevant to all three objectives. An improved understanding of the structure of the upper atmosphere is required for a better understanding of escape processes, which play a key role in atmospheric evolution. It will also provide information on the current upper atmospheric densities, of importance 2 months later when the Mars Observer arrives and will use aerobraking to achieve orbit around Mars.

Pathfinder ASI/MET measurements should also yield information pertinent to the general circulation on dust storms, thermal tides, transient baroclinic eddies, the Hadley circulation (including possible "western boundary currents"), slope flows, gravity waves, regional circulations, and small-scale phenomena (e.g., dust devils). New types of atmospheric phenomena might also be observed. The much greater resolution of the Pathfinder pressure data (relative to Viking) may enable differentiating normal modes from tides, and permit a much better detection of mesoscale and smaller-scale phenomena than was possible with Viking, although enhanced modeling capabilities will probably be critical for this.

Vertical Structure of the Atmosphere

Entry Measurements

During its entry into the atmosphere of Mars, the deceleration of Pathfinder will be measured as a function of time. From these data, the atmospheric density, pressure, and temperature will be derived as functions of altitude, as discussed by *Seiff* [1976] and done by *Seiff and Kirk* [1977]. Significant differences between Pathfinder and Viking will, however, affect the specific approach to atmospheric definition. (1) Viking was three-axis stabilized; Pathfinder is aerodynamically stabilized and spinning. (2) The Viking entries were lifting entries from Mars orbit at 4 km s^{-1} with very shallow path angles; the Pathfinder entry is direct from the deep space approach trajectory, ballistic, and at a steeper angle and a higher velocity, 7.5 km s^{-1}, than Viking. (3) The Viking landers carried three-axis gyroscopes to define angular rates of the spacecraft; Pathfinder does not. (4) Viking was able to deploy sensors outside the lander boundary layer body in parachute descent; Pathfinder will not.

The velocity and flight path angle, γ, relative to horizontal, expected on the Pathfinder entry trajectory are shown in Figure 3 as functions of altitude. Velocity is nearly constant above 60 km, owing to the minimal drag at these altitudes, and the accelerating effect of gravity. The Pathfinder entry experiment will begin at an altitude determined by the accelerometer sensitivity, which is 2 μg (micro g's) on its most sensitive range. Given the spacecraft mass and frontal area, the threshold atmospheric density measurement is estimated to be ~2 × 10^{-10} kg/m^3. This density occurred in the Viking atmosphere profiles at an altitude of ~150 km.
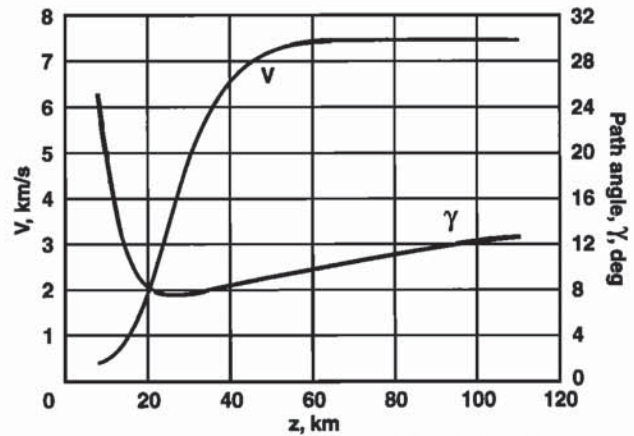

Figure 3. The Mars entry trajectory of Pathfinder. The spacecraft enters the atmosphere with a velocity of 7.5 km s^{-1} at a path angle 12° below the horizontal. Strong deceleration begins at about 50 km altitude. At 20 km the path angle starts to steepen, reaching 25° at 8 km, where the parachute is deployed. Velocity has then decreased to sonic.

Accelerations will be read 32 times per second during entry and, to establish their offsets or readings at 0 g at the time of entry, will also be read a few minutes before entry. Data taken must be stored in memory because of an anticipated communication blackout during entry resulting from ionization in the vehicle shock layer, and will be transmitted to Earth soon after landing and antenna erection. Altitude resolution is determined by the sampling rate and the lander descent velocity, $V \sin \gamma$. Resolution is ~50 m at and above 100 km altitude, and improves as descent velocity decreases, reaching 5 m at parachute deployment. This resolution should permit the study of oscillatory features as small as ~250 m to 25 m in depth.

The density is derived from

$$\rho = (2m/C_D A)a / V^2 \qquad (1)$$

where m and A are the mass and frontal area of the spacecraft, a the measured deceleration, and C_D the drag coefficient. The drag coefficient is already well established from the Viking work, which used the same body shape [*Seiff and Kirk*, 1977]. To define the history of velocity V, altitude z, and flight path angle γ, it is necessary to reconstruct the trajectory, using the equations of motion, the measured accelerations, and the initial velocity and path angle at entry [*Seiff and Kirk*, 1977]. The altitude relative to the surface is then calculated from

$$z = z_f + \int V \sin \gamma \, dt \qquad (2)$$

where z_f, the altitude at parachute deployment, is established by the descent mode measurements. Pressure is obtained from the density profile through the assumption of hydrostatic equilibrium,

$$p = -\int \rho \, g \, dz \qquad (3)$$

Temperature is obtained from the equation of state, given the atmospheric mean molecular weight established by Viking. These techniques have been applied in the atmospheres of Mars, Venus, and Jupiter [*Seiff et al.*, 1980, 1996].

Accelerometers. The accelerometer configuration on Pathfinder is shown in Figure 4. To place the sensors near the spacecraft center of gravity (c.g.) during entry, they were mounted on an aluminum plate located as the central board in the
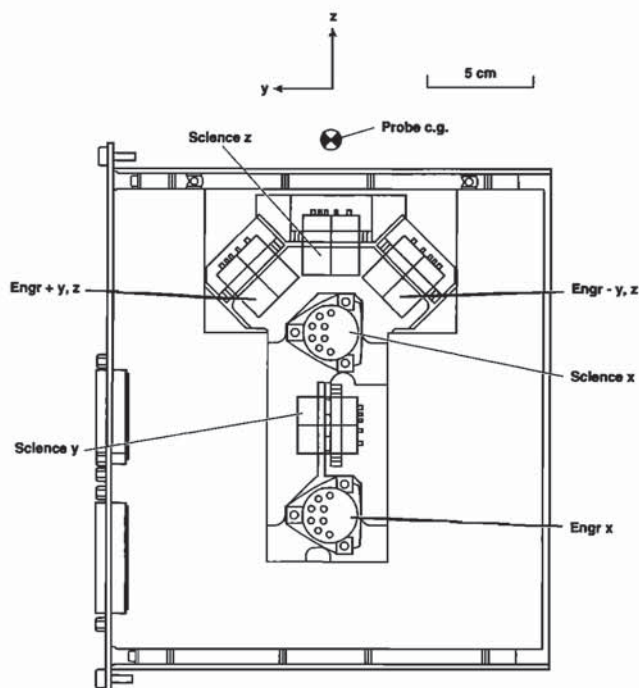
Figure 4. The accelerometers are mounted on a stiff aluminum plate located at the center of the integrated electronics unit. This places the test masses on the spacecraft z-axis, the longitudinal axis of symmetry. The center of gravity (c.g.) of the entry configuration shown is presently uncertain by ±2.5 cm. Science and engineering z-axis sensors are nearest the c.g. Science y-axis and engineering x-axis sensors, being more remote, are subject to larger angular acceleration inputs.

"integrated electronics unit." The three science accelerometers are aligned with the spacecraft x, y, and z axes, where z is ideally the axis of symmetry of the lander heat shield, and x and y are normal to that axis, y in the plane of the sensor mounting plate. The sensor test masses (sensitive elements) lie along the entry z axis and are a few centimeters away from the lander c.g. They are therefore subject to inputs from angular accelerations resulting from lander pitching and yawing motions and may require correction for these inputs. For independent lander purposes, a second set of three "engineering accelerometers" is mounted on the same plate with the science sensors. Two of these measure the resultant of z and y acceleration components, from which a_z and a_y can be calculated. Data from these sensors will be available to aid in interpretation and correction for angular inputs to the science measurements.

All six accelerometers, three science and three engineering, are Allied Signal QA-3000-003 units. They measure acceleration by measuring the electromagnetic force needed to hold a flexure-mounted test mass in a fixed, null position in a permanent magnetic field. The restoring force is provided by current in a coil within the test mass, and the current is the measure of the acceleration. Each accelerometer signal channel has three gain states with dynamic ranges of 40 g, 800 mg, and 16 mg. Signals are digitized to 14 bits to provide resolutions of 5 mg, 100 μg, and 2 μg on the respective ranges. During testing, noise levels in each gain state were measured at 1 to 2 counts or less, which implies that accelerations of 10 μg should be significant with 20% uncertainty. The accelerometers are designed to measure entry

vehicle deceleration from the limits of detectability to a maximum of roughly 27 g at 30 km. Low-pass filters in the accelerometer electronics attenuate signal frequencies above 5 Hz to suppress the effects of noise and spacecraft dynamic motion.

The primary function of the engineering accelerometers is to set the time of important events during entry and descent, particularly parachute deployment. They are also used after landing to right the spacecraft and point the lander high gain antenna accurately. Science accelerometer observations focus on measuring atmospheric accelerations throughout entry and descent with maximum resolution, although the optimum measurement strategy has been modified to provide redundancy for the engineering accelerometers. Data from all six accelerometers are sampled at the same rate and will be usable for science purposes.

Calibration. Accelerometer calibration measurements were made to define end-to-end response for each sensor and also to establish alignment and location relative to the lander spacecraft coordinate system. End-to-end response measurements used the assembled flight accelerometer board (Figure 4) on a precision dividing head to establish the linearity, gain, and offset at each gain setting over a temperature range of –5°C to +40°C. The sensors are highly linear, and gains and offsets vary linearly with temperature. Calibration measurements are limited to 1 g on the 40 g gain setting and have not covered the full temperature range expected for the electronics, so that some extrapolation is required. These measurements have established the relative orientation of the accelerometers in the flight board coordinate system to ~0.0005 rad.

Calibration measurements with the accelerometer board installed on the spacecraft have also established the orientation of the sensors to ~0.0005 rad in the lander coordinate system. Further optical measurements on the spacecraft in its cruise configuration have established the shape of the heat shield and the orientation of its symmetry axis in the spacecraft coordinate system with similar accuracy. The relative orientation of these two coordinate systems will not be measured, but they are specified to be coincident to better than 0.0044 rad and are expected to be considerably better in practice. During the spin balancing of the spacecraft, the location of each sensor relative to the entry vehicle c.g. will be determined to about 2 mm in the x and y directions. In the z direction the location of the c.g. will not be measured and will be uncertain to approximately 2.5 cm.

Parachute Descent Measurements

During parachute descent from ~8 km to the surface, atmospheric pressure and temperature will be measured as functions of time at 2 samples/second (sps), giving altitude resolution of nominally 50 to 100 m. The same pressure sensor will be used in this mission phase and after landing. It is described in the following section. The temperature sensor is of similar design to those used after landing, but because of mounting and location requirements, is used only for this mission phase.

These sensors are mounted just inside the lander, in one of the three triangular "window" openings formed by two adjacent solar panels and the base petal of the lander in the petals-closed configuration, as shown in Figure 5. Ideally, the sensors would be located outside the lander boundary layer in a region of high-velocity flow in order to assure accurate sampling of the atmosphere [Seiff, 1976]. This was not done because of a spacecraft constraint on projections outside the lander body, which could possibly puncture the air bags during inflation and thus jeopardize a safe landing. The importance of location for temperature
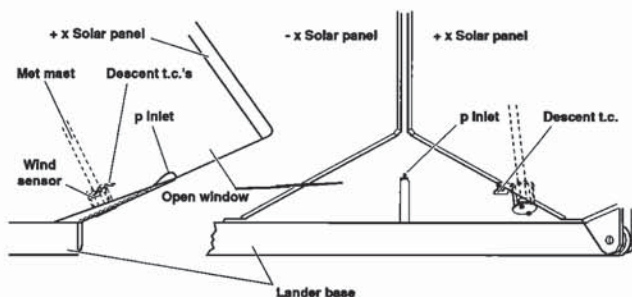
Figure 5. Sketch of pressure inlet and descent thermocouple locations during parachute descent. The pressure inlet lies in the plane of the triangular window opening at one corner of the lander. (The sensor itself is on the lander base near the integrated electronics unit box.) The descent temperature sensor is just below the wind sensor on the stowed meteorology mast, oriented approximately parallel to the window opening.

sensing is that the sensor must not be thermally contaminated by the spacecraft and should be well coupled thermally to the atmosphere. Thermal contamination can arise by radiative exchange with warm spacecraft elements, or by sampling atmospheric gas that has exchanged heat with the spacecraft. Thermal coupling is important in that high convective heat transfer from the atmosphere to the sensor, promoted by high gas velocity through the sensor, gives short response time and minimizes errors due to extraneous heat inputs [*Seiff*, 1976]. Since pressure varies with location around the periphery (and within) a descending spacecraft, orientation of the pressure inlet relative to the gas flow, and the relationship of pressure measured to that in the ambient atmosphere must be known to interpret the data.

It thus became necessary to know the flow conditions at the sensor locations within the lander. Tests of a lander model in the Mars wind tunnel (operated by Arizona State University at Ames Research Center). indicated that there is no organized flow through the triangular "window" opening and through the lander interior. Instead, there is a pulsating, turbulent motion of gas at the sensor locations, sometimes inwardly directed, at other times outwardly directed. The magnitude of the mean velocity past the temperature sensor is from 0.1 to 0.3 times descent velocity, which implies poor thermal coupling. Outward directed flow probably includes gas warmed by thermal contact with the spacecraft interior. A report of the wind tunnel tests has been submitted for publication (T. Rivell et al., Low-speed wind tunnel tests of the internal flow through the Mars Pathfinder lander, submitted to *Journal of Spacecraft and Rockets*, 1996).

The quantitative consequences of these unfavorable sensor locations on the atmospheric measurements in parachute descent are not presently known. Pressures measured may differ from ambient by as much as the dynamic pressure, $\rho V^2/2$, where ρ is ambient density and V is the descent velocity. For near-surface conditions, $\rho = 0.01$ kg/m^3 and $V = 100$ m s^{-1}, this defines an uncertainty of up to ± 0.5 mbar. Effects on temperature are difficult to estimate from present knowledge. However, the effects may be smaller than anticipated. It may become possible to quantify the errors and devise corrections to the measurements. It is presently difficult to appraise the usefulness of data from this mission phase.

Landed Meteorology Measurements

After Pathfinder lands and erects the MET mast, temperature will be sensed at three heights above the surface, pressure at the surface, and wind speed and direction 1.1 m above the surface. Sampling sequences are flexible, being controlled by ground command. The nominal schedule assumed in instrument design was sampling of the sensors at 4-s intervals for 5 min of every hour, with 1 hour of continuous data once per day in the afternoon. The sensors are described below.

Pressure Sensor

The ASI/MET pressure sensor is a Tavis deflecting diaphragm, variable reluctance sensor, similar to Viking lander pressure sensors [*Chamberlain et al.*, 1976]. Although relatively massive, it was selected for its reliability and excellent repeatability, apparently 0.07% between two years on Mars [*Tillman et al.*, 1993]. The sensors demonstrated stability and reliability over several years of operation on Mars.

As noted above and shown in Figure 5, the inlet lies in the plane of the aperture between the lander instrument shelf and two petals in the descent configuration, and was oriented perpendicular to the anticipated airflow during descent. It is connected to the sensor by approximately 1 m of 2 mm inside diameter tubing. The tubing limits response time to 1.5 s at 3 mbar and 0.45 s at 10 mbar.

Two pressure ranges are provided; 0–12 mbar for descent and 6–10 mbar for surface observations. Both ranges are read in each data session. This provides the capability of reading surface pressures >10 mbar if needed. Amplification and biasing of the same signal provide the two different outputs. Resolution at 14-bit digitization is 0.75 μbar and 0.25 μbar resolution, respectively, 120 times finer than Viking measurements. The 0 to 5 V signal is digitized by the same 14-bit analog to digital converter as all other meteorology sensors. System noise levels were measured at <2 counts, i.e., <1.5 μbar.

Tavis pressure sensor measurements are moderately temperature dependent. To permit temperature corrections, the sensor temperature is monitored by a platinum resistance thermometer (PRT) over the temperature range, 200–335 K, with a resolution of 0.01 K.

The flight sensor was calibrated against an accurate Baratron gauge in a vacuum chamber in 2-mbar steps between 0 and 12 mbar at temperatures of –80, –40, 0, and 20°C. The maximum difference among the calibrations over the temperature range was approximately 0.18 mbar at zero pressure and 0.036 mbar at 12 mbar, corresponding to 1.8 and 3.6 μbar/°C. The temperature sensor within the pressure sensor assembly will assist in correcting this temperature sensitivity to the extent it is repeatable. In addition, the gain and offset of the pressure sensor electronics have been measured accurately for both pressure channels at ambient temperature (22°C).

The sampling strategy for pressure is simpler than for temperature and wind because the large-scale phenomena which affect pressure are slowly varying. Fast sampling for pressure consists of samples or averages at intervals of the order of 1 to 10 min. The Viking studies were based on hourly averages of mostly single-point measurements separated by 17 to 37 min and sometimes an hour. Since we have much better measurement resolution, it could prove valuable to sample at higher rates at times. Since pressure sampling is tied to sampling of the other meteorological variables, this will be automatically accomplished.

To measure atmospheric normal modes, diurnal harmonics, etc., the same basic sampling interval, approximately every hour, will be used day and night. Averaging several samples to reduce noise or increase statistical reliability is not as necessary as for temperature and wind. Pressure measurements are independent of
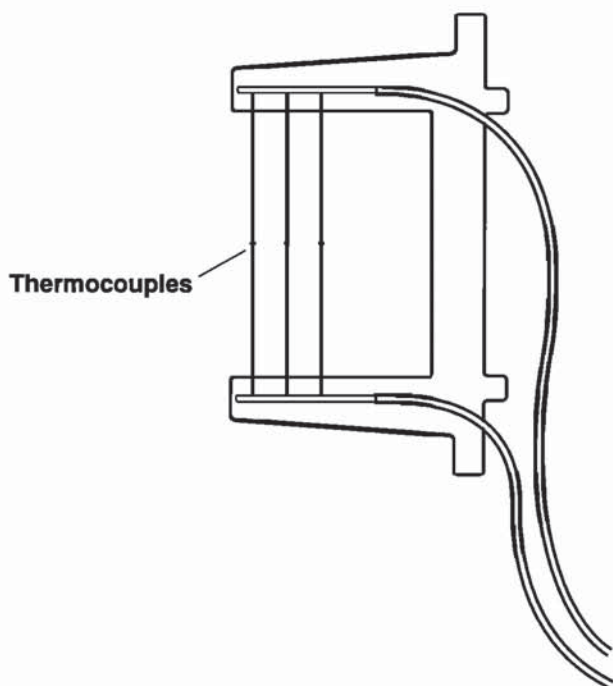
Figure 6. Mounting configuration of the temperature sensing thermocouple triads. With three sensors in parallel, two can be broken without loss of data.

other measurements and are not sensitive to flow over the lander at low wind velocities.

Temperature Sensors

The Mars Pathfinder MET temperature sensors are designed to provide reliable, time-resolved measurements of the atmospheric kinetic temperatures and their vertical gradients near the Martian surface. Accurate measurements of these quantities are a challenge in the thin, low-heat-capacity atmosphere of Mars because the thermal coupling between the sensor and the atmosphere is weak, while sources of thermal contamination (solar and thermal radiative heating of the sensor elements, and conduction to the support structure) are still present. In these conditions, many conventional temperature sensor types used for terrestrial meteorology operate more as bolometers than kinetic temperature sensors. In addition, as the atmospheric heat capacity decreases, the time required for the sensor to equilibrate with the atmosphere increases, reducing the time resolution and adding ambiguities to the analysis of results obtained in rapidly changing conditions, like those anticipated near the Martian surface.

Thin-wire thermocouples (TCs) were chosen for the Pathfinder application because those used on Viking appeared to provide adequate durability, accuracy, and response time. This sensor type is also much less susceptible to calibration changes due to stretching or dust abrasion than thin-wire resistance thermometers.

As on Viking, each ASI/MET TC assembly includes three, 75-μm (0.003 inch) diameter chromel-constantan (E-type) thermocouples suspended across a 2.38-cm gap between the arms of a C-shaped fiberglass-epoxy bracket (Figure 6). The separation between the thermocouple leads is 0.3 cm. The fine wires provide conductive isolation for the junctions and ensure that they reach equilibrium with the tenuous Martian atmosphere fairly rapidly. On the surface of Mars the thermocouple junction time constant

is of the order of 4–5 s at a wind speed of 1 m s^{-1}, decreasing to 0.6 s at 50 m s^{-1}.

The three TCs in each assembly are wired in parallel to increase their output current and to preclude a complete failure unless all elements are broken. Unlike the Viking thermocouples, which were butt-welded to minimize the size of the TC junction, the Pathfinder TC junctions were welded with the chromel and constantan lead wires side-by-side, and then straightened. This approach produced a somewhat larger (200 μm) junction. These larger junctions increase the response times. Also, the Pathfinder fiberglass TC mounting brackets are not coated with a low-absorption material and may therefore contribute to radiation errors of the ASI/MET temperature measurements. Radiative corrections will have to be modeled to obtain the best results from these sensors.

Because thermocouples are differential temperature sensors, a reference junction with an absolute temperature sensor, an accurate PRT with a range of 140 to 330 K and a resolution of 0.01 K is an integral part of this system. Each thermocouple has a dynamic range of roughly 100 K about the PRT temperature and a resolution of 0.01 K. The reference junctions for each of the three MET TCs and the ASI descent TC are at the junctures of the thermocouple wires to copper wires on individual $4 \times 8 \times 1$ mm thick alumina (Al_2O_3) junction blocks. These junction blocks were thermally coupled on an aluminum block to minimize thermal gradients across and between the junction blocks. This isothermal block "cold junction" (CJ) consisted of a machined $1 \times 2 \times 4$ cm aluminum bar with covers to enclose the individual alumina junction blocks. The temperature of the junction block is measured with a thin-film PRT (Rosemont 118ALK2) mounted in a small cavity at the center of the aluminum bar. This block is mounted at the base of the MET mast.

Sensors for both the descent and landed phases of the mission are mounted on the MET mast. A single TC set is assigned to temperature measurements during the descent phase of the mission, when the entry vehicle is descending on the parachute. The descent sensor is located on the meteorology mast just below the wind sensor. Its TC wires are approximately 4 cm from the mast axis and are oriented perpendicular to it. With the mast in stowed position during descent, the sensor is near one corner of the lander aperture and is also set back from the opening significantly, owing to its position below the wind sensor.

The three TC sets for temperature measurements during the landed phase of the mission are located on the deployed mast 0.25, 0.50, and 1.00 m above the plane of the solar petal. For each sensor the TC wires are oriented vertically approximately 2.3 cm from the mast axis. The three sensors and mounts are identical and are clocked at the same angle on the mast. Temperature measurements are subject to thermal contamination when the mast is downwind from the spacecraft or the sensor wires are downwind from the mast. The sensors are therefore oriented away from the spacecraft when the mast is deployed, so that these conditions coincide, minimizing the range of unfavorable wind directions.

The output voltage produced by chromel-constantan TCs varies from −6.516 mV at 143.15 K to about +1.801 mV at 303 K, referenced to a 0°C cold junction [*OMEGA*, 1991]. The TC voltage is amplified before being read out by the ASI/MET multiplexer and 14-bit analog to digital converter (ADC). An OP177 operational amplifier was used for this application, providing a gain of approximately 475. With this gain, the 14-bit ADC provides a resolution of 0.01 K.

To calibrate the ASI/MET temperature sensors, each TC assembly was mounted in a copper enclosure that was placed inside a test chamber with a dry nitrogen environment at ambient pressure. The temperature of the chamber was controlled over the range 140 to 360 K and monitored with National Institute of Standards and Technology (NIST)-traceable thermometers. The largest gradients measured across the copper enclosure were less than 0.01°C. The cold junctions also were placed in the test chamber, but they were mounted outside the copper enclosure, and their temperatures could be controlled independently.

To provide an end-to-end calibration of the ASI/MET TCs, the flight electronics were used to record the TC output voltages as a function of chamber temperature. The measured voltages were then converted to temperature for comparison with the standard thermometers, with the aid of a fifth-order polynomial fit to a published voltage versus temperature curve for chromel-constantan TCs. These conversions sometimes produced discrepancies as large as 0.2°C, but these discrepancies varied smoothly and were repeatable to an accuracy of 0.01°. A more detailed calibration of these sensors was not possible because the resistance of the TC leads was not measured. The time constants of the sensors were not measured, but were estimated for Mars ambient conditions from correlations of heat transfer to fine wires. As noted earlier, they depend strongly on wind velocity ranging from 4 to 5 s at 1 m s⁻¹ to 0.6 s at 50 m s⁻¹.

The end-to-end temperature calibration was performed with the flight electronics at ambient temperature. To correct for electronics board temperature variations expected during the mission, the response of each of its channels to fixed input voltages was measured over the –40°C to 50°C temperature range, allowing accurate gain and offset temperature coefficients to be derived. For the thermocouple channels, gain is also dependent on lead resistance. This effect was present in the end-to-end calibrations but was not part of the electronics gain measurements. Lead resistance for each thermocouple was therefore measured at ambient temperature using an alternating current technique to eliminate errors produced by thermocouple voltages.

The goals of the ASI/MET TCs were to provide absolute accuracies of 1 K, relative accuracies of 0.1 K, and resolutions of 0.04 K at temperatures between 160 and 300 K. Results presented above indicate that the TC electronics can achieve these accuracy and resolution goals. The actual performance of these sensors in Martian conditions will depend on other factors that are not yet known, including the sensor response to solar and thermal radiation. Barring mechanical accident, these sensors should have no difficulty exceeding the design lifetime of 30 days, with a goal of 1 year.

Like other ASI/MET instruments (besides the accelerometer), the TCs will be sampled eight times each second, but only one sample out of four will be retained, yielding an effective sampling rate of 2 Hz. This sampling time is expected to be usually shorter than the response time of the sensors.

Wind Sensor

There was no wind sensor in the original plan for the ASI/MET. In early meetings, the Science Advisory Team discussed the important capability that would be added to the instrument by a simple wind sensor. A specific concept for this sensor was proposed, developed, and demonstrated in tests at Ames Research Center, approved, and implemented by the Jet Propulsion Laboratory (JPL) instrument team.

The sensor is composed of six identical hot-wire anemometer elements of 0.9 Pt/0.1 Ir alloy, 65-μm-diameter wire arrayed around a circular cylinder 2.7 cm in diameter (Figure 7). The six elements are in series and carry a common heating current. The wires are wound around insulating posts and positioned ~3 mm away from the cylinder surface, as shown in the cross section. When exposed to wind, the overall cooling of the sensor wires depends on the wind velocity, while the six different segments experience cooling differences which depend on the wind direction. Maximum cooling occurs at about 45° from the windward meridian.

In operation, a continuous current of 51.5 mA, dissipating 0.38 W, heats the elements ~40°C above ambient temperature in still CO_2 at typical Martian surface pressures. (The design was power constrained; a larger overheat would have been desirable.) With wind blowing, the wire temperatures decrease, and the wind is measured by the temperature rise above that for zero current. Wire temperature changes are accompanied by wire resistance changes and are measured by the voltage drops across each segment. A set of six voltages and the heating current thus comprise a data sample. In addition, it is important to determine the temperature of each element at zero heat input as well as with the heating current flowing. This is done by operating intermittently in a low power mode, 20.6 mA for 3 ms, which does not raise the temperature measurably. Temperature measurement resolution is 0.11°C for low power and 0.04°C for high power operation.

The thermal response of the individual segment anemometers to wind flow depends on the local fluid velocity at their meridional stations. Local flow velocity in the flow field of a cylinder in a transverse gas flow is a function of meridional angle θ and radial distance r from the cylinder surface. Velocity is zero on the windward and leeward meridians, where the flow is stagnant. On the front half of the cylinder, velocity increases with meridian angle and decreases with distance from the surface. Near the maximum diameter station, depending on the Reynolds number, the flow separates from the surface and forms a viscous wake,
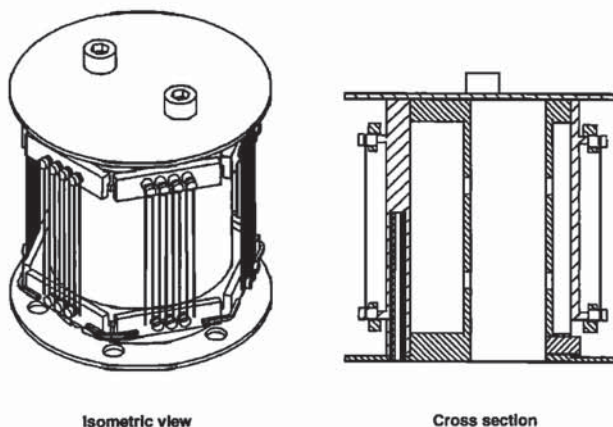

Isometric view   Cross section

Figure 7. MET wind sensor. Four of the six hot wire anemometer units are visible in the isometric view. The cross section shows the fine wires which are wound around nylon pins and stand off about 3 mm from the circular cylindrical core. The hole in the thick left wall of the cylinder is the insertion hole for the thermocouple which monitors cylinder temperature. The oversize top and bottom plates constrain the fluid from spilling over the cylinder ends and thus promote two-dimensional flow.

within which fluid velocities are low and, at $\theta = 180°$, reverse in direction. These variations control the distribution of cooling among the six anemometer elements.

The heat transfer coefficient h ($W/cm^2 K$) of a single wire in transverse flow varies, to first order, as $u^{0.5}$, where u is the flow velocity. Wire temperature rise, ΔT, is inversely proportional to the heat transfer coefficient, being governed by the requirement that the temperature rise at equilibrium is just that needed to transfer the electrical heat input P (watts) to the atmosphere:

$$h\Delta T = P \tag{4}$$

or

$$\Delta T \sim P/u^{0.5} \tag{5}$$

To evaluate this sensor concept, two development models were built and tested at 12-mbar ambient pressure in the Mars wind tunnel at Ames Research Center. The first, a simple planar array of 0.1-mm-diameter wires placed normal to the flow, was used to establish correlation with the fine-wire heat transfer correlation of *Baldwin et al.* [1960]. The data agreed with the correlation within graphical comparison accuracy (~10%). The second model was a prototype of the cylinder configuration and showed good sensitivity to wind direction and magnitude. Heat transfer to individual wires of this sensor, compared to the Baldwin and Sanborn correlation using computational flow analysis to define the local velocity field, agreed with their graphical correlation, again within plotting accuracy. At Mars surface conditions and low air speeds, slip flow occurs on the wires, and dimensionless heat transfer coefficient is no longer a function of Reynolds number only. A second parameter, Mach number, is introduced by Baldwin et al. into the correlation in lieu of Knudsen number, the ratio of mean free path to wire diameter, which is the actual determinant of the flow regime.

With the operating principle and wind measuring sensitivity confirmed, a nominal design for the flight sensor was selected. The mechanical and the electronic design and construction were carried out by the instrument team at JPL. Three nominally identical units were constructed and subjected to end-to-end temperature calibration measurements. The first was mounted on the flight mast, the second was held in storage as a flight spare, and the third, designated the science test unit, was delivered to the Ames Research Center for wind calibration. The total resistance of the six elements in the science test sensor is 141.16 ohms at
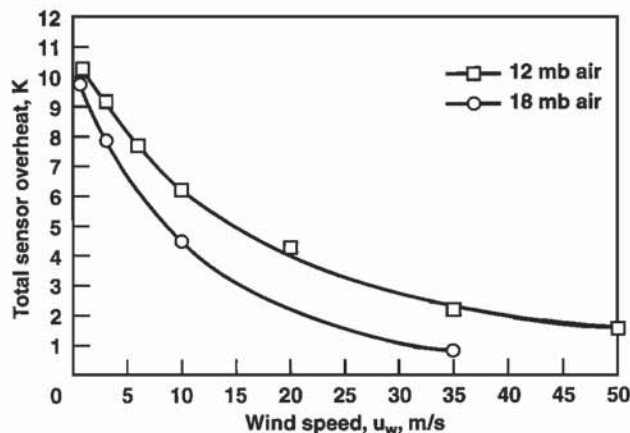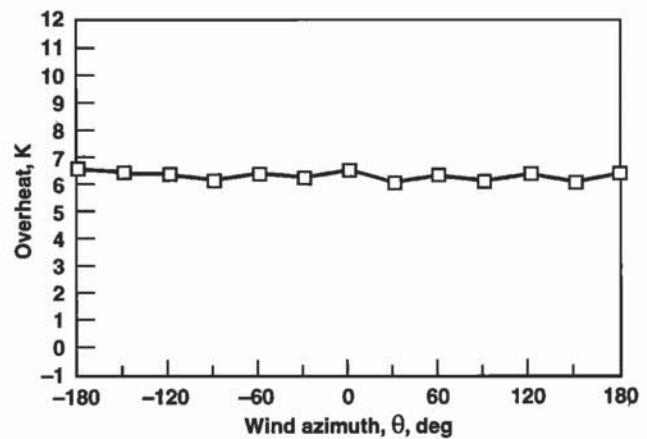

Figure 9. The variation in total sensor overheat with wind direction is small, ~0.25° amplitude for the conditions shown. This is an important property of the sensor, since it permits wind magnitude to be measured independent of wind direction.

21.7°C. Sensor segment resistances vary by up to 2.2%. Thus the segment resistances must be accurately measured to define the wind direction.

The science test unit was calibrated in the Mars wind tunnel. This facility is capable of simulating Mars atmospheric conditions with air or CO_2 at wind speeds from 0 to 150 m s^{-1} [*Greeley et al.*, 1977]. Initial tests were in air at densities of 0.010, 0.015, and 0.0225 kg/m^3 to simulate surface densities of Mars' atmosphere. Corresponding air pressures were 8, 12, and 18 mbar. Wind speeds ranged from 0 to 50 m s^{-1}, and wind directions from 0 to 360° in steps of 30° and 0 to 60° in steps of 5°. Wind direction changes were simulated by rotation of the sensor in the wind tunnel. The wind measurement standard was a laser interferometer velocimeter manufactured by TSI, Inc., which measures the velocity of micron-size dust particles introduced into the air stream. It is accurate to within 0.5% of reading, or 0.05 m s^{-1} at 10 m s^{-1}. This device measured and reported the mean wind speed and statistics on the distribution of velocities about the mean.

Four questions were addressed in the calibration. (1) What is the total sensor overheat under zero-wind conditions? (2) How does the total sensor overheat vary with wind speed? (3) What is the sensitivity and resolution of the sensor for wind direction? (4) What is the response time of the sensor to changes in wind speed?

The sensors were initially tested at vacuum to evaluate the power loss due to conduction to the wire supporting structure and radiation to the environment. These must be subtracted from the total power input to obtain power lost by convection. The input power at vacuum was found to increase linearly with wire temperature, indicating that conduction is the primary loss mechanism. Blackbody radiation calculations also indicate the sensor heat loss due to radiative emission is minimal.

Under wind tunnel air flow conditions at 12 mbar, the sensor attains equilibrium temperatures within ~1 s after power is turned on. As expected, the total sensor overheat decreases with increasing wind speed as shown in Figure 8. The variation is not as simple as indicated by (5) because of a number of factors including the effect of increasing Reynolds number with increasing wind speed on cylinder boundary layer thickness and local velocity ratios, while velocities in the separated flow region are

Figure 8. Sensor temperature rise (overheat) as a function of wind velocity with nominal heater power, 0.38 W. Tests were in air near room temperature at pressures of 12 and 18 mbar.

less sensitive to wind velocity than those on the forward region of the cylinder. Calibration is thus essential. In analysis of the data, overheat is always defined by the temperature difference of the same sensor element at the high and low power levels. If short-term atmospheric temperature changes are encountered, the wind measurement will rely on the concurrent sampling of atmospheric temperature by the upper MET thermocouples to indicate these changes.

The decrease in sensor overheat with increasing wind speed is quasi-exponential with an *e*-folding rate of ~22 m s^{-1}, so that at 50 m s^{-1} the overheat is ~1 K. Under anticipated wind speeds of generally <20 m s^{-1} seen at Viking Lander 1 site during the Pathfinder season [*Murphy et al.*, 1990], typical sensor overheat should be >5 K.

The total sensor overheat exhibits only a slight variation with wind direction for a given wind speed, with the greatest variation (~1 K) at higher wind speeds. When a segment of the sensor is directly upwind, the total sensor overheat is greater in the low-velocity stagnation region than when the upwind direction is midway between two sensor segments, where local flow velocity is higher. The magnitude of this difference is shown in Figure 9 for a wind speed of 10 m s^{-1}.

On Mars, corrections for solar radiative heating may be required. Also, for prolonged operation, the cylinder core becomes warmer than the atmosphere, and correction for its radiation may be necessary. A single chromel-constantan TC junction is mounted within the wall of the wind sensor core to provide a basis for this correction.

To distinguish wind direction, the overheats of the six segments are compared. The maximum segment overheat occurs downwind of the sensor where there is a broad angular range of low velocities, while the minimum overheat occurs at ~45° from the upwind point of the sensor. Thus segments on the downwind portion of the sensor will be warmer than those on the upwind side (Figure 10).

Just as the total sensor overheat is a function of the wind speed, so too is the difference between the maximum and minimum segment overheat at a given wind speed, as may be seen in Figure 10. The minimum difference, $\Delta T = 0$, occurs of course,
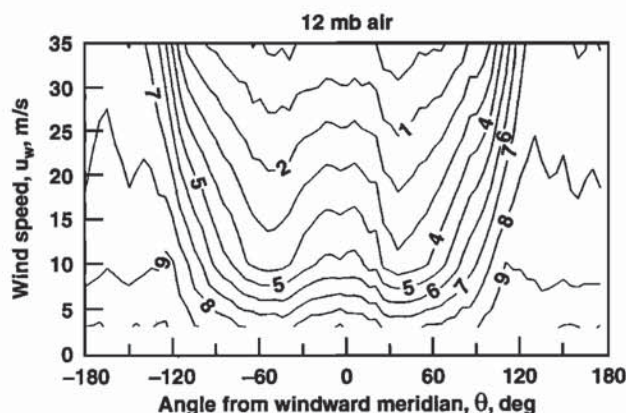
under zero wind conditions. As wind speed increases, ΔT increases to 2.4 K at 3 m s^{-1}, 5.5 K at 10 m s^{-1}, reaching asymptotically a maximum of ~8 K beyond 20 m s^{-1}. Thus comparison of the individual segment overheats themselves can provide an estimate of wind speed as well as wind direction.

Figure 10 shows contours of constant segment overheat as a function of wind speed and segment angular position relative to the upwind location. (The angle $\theta = 0°$ represents the upwind location.) At $\theta = \pm 120°$, segment overheat decreases from 10 K at 3 m s^{-1} to 2 K at 35 m s^{-1}. Additionally, the smallest segment overheat at any wind speed occurs at ~$\pm 45°$. The angular interval across which the overheat most rapidly changes moves toward the rear of the sensor with increasing wind speed. The variation in overheat over the angular interval within 60° of the sensor's downwind point ($\pm 180°$ in Figure 10) is <1 K for wind speeds up to 25 m s^{-1}.

The flight sensor was not calibrated in the wind tunnel because of the possibility of damaging it in handling and because it would be contaminated by the fine dust used to measure wind speed in the tunnel. The temperature calibration of the flight sensor (measurements of element resistance as a function of temperature) was conducted at the same time as the TC and PRT temperature calibration discussed above. End-to-end temperature calibration of element resistances as a function of temperature was performed from 140 to 360 K as well as flight electronics gain and offset calibration over the range –40°C to 50°C. In addition, the constant currents supplied by the flight electronics to heat the wind sensor windings were measured accurately in both low and high power modes at ambient temperature. The temperature dependence of gain and offset are very similar for all six channels. The science test and flight sensors are nominally identical, so the science test unit wind tunnel calibration should be applicable to the flight unit. The geometric tolerances for the sensors have been documented and are on file, in case it becomes necessary to consider possible calibration differences between them. Calibration of the science test unit in 0.9 CO_2/0.1 air has also been recently performed, and is being analyzed at this writing. Initial indications are that it is very close to the calibration in air.

Testing of the Pathfinder ASI/MET wind sensor indicates that the sensor is capable of measuring wind speed to within ~1 m s^{-1} at low wind speeds and within ~4 m s^{-1} above 20 m s^{-1}, assuming an accuracy of 0.25°C in overheat measurement. The sensor should detect wind directional variations as small as 10°.

Data Handling and Mission Operations

Data will be collected from the MET instruments 5 min out of every hour around the clock, unless limited by available power. In addition, continuous sampling during 1 hour each afternoon is requested and is expected to be available. The afternoon is when spacecraft power is most available.

All sensors, temperature, pressure, and wind, are read every 0.5 s and averaged for telemetry every 4 s, but a point-sampling mode (no averaging) is also available on ground command. Housekeeping data are averaged for 32 s and sent down at every eighth data sample.

Reference temperatures, including thermocouple "cold junction" temperatures are treated as housekeeping data. More frequent sampling of these is not considered necessary, since these readings are not expected to fluctuate on a short timescale.

Flexibility has been built into the hardware systems to permit variation in sampling strategies. The ASI/MET Science Team

12 mb air

Figure 10. Contours of constant element overheat in wind speed, wind direction space. The angle $\theta = 0$ corresponds to the windward meridian. Maximum overheat occurs on elements in the base region of the cylinder, where the flow is separated and velocities are low. Minimum overheat, which corresponds to maximum airstream cooling, occurs about $\pm 45°$ from the windward meridian. This distribution is the basis for determining wind direction.

and the Project Science Team will meet frequently to review and discuss latest results and findings and to select scientific emphasis, including sampling strategy, for the following days. Thus Pathfinder mission operations will be a highly interactive process.

Operational flexibility is provided by the spacecraft attitude and information management subsystem, which controls instrument operation through a limited set of commands. It selects, samples, and processes the instrument data streams, constructs data packets for downlink, and directs data to the spacecraft engineering, housekeeping, and accountability data stream. Data from all lander spacecraft subsystems, including the accelerometer and MET instruments, are directed via the lander interface assembly to the lander remote engineering unit (LREU). Whenever they are turned on, data from the accelerometer and MET instruments are sampled continuously by the Pathfinder spacecraft to a schedule defined by a single LREU table. With the exception of the six accelerations which are sampled 32 times per second, all the measurements are sampled eight times per second, but only every fourth measurement is retained and used for determining averages and variances.

Concluding Remarks

An instrument on the Pathfinder Mars lander is designed to measure the structure of Mars' atmosphere during entry and descent, and near-surface meteorological parameters over a period from 30 sols to one Earth year after landing. The instrument appears capable of obtaining information on the current structure of Mars' upper and middle atmosphere and of yielding significant new information on the meteorology. Measurements will include the temperature profile of the near-surface atmosphere. A new wind sensor was devised which should yield useful magnitude and directional information in the velocity range up to at least 20 m s^{-1}, with an upper limit of 50 m s^{-1}.

Appendix: Brief Historical Note

A proposed mission which preceded Pathfinder was the Mesur multi-probe mission to Mars, which was to deliver 20 small probes distributed over the planet to perform geochemistry, geology, seismology, and meteorology experiments. The NASA Office of Space Sciences appointed a Science Definition Team for this mission, which met between February 1991 and June 1993. Among the conclusions of this team was a recommendation that each of the probes on this proposed mission carry an atmosphere structure instrument and a meteorology package. The emphasis in the latter was on pressure measurement at multiple sites.

The Pathfinder spacecraft was originally proposed as a demonstration of the Mesur probe concept, so this recommendation was carried forward to Pathfinder. At the project outset in 1993, atmospheric measurements planned were, however, minimal. An instrument to measure structure of the atmosphere during entry and descent would use techniques similar to those employed on the two Viking entries. After the landing, the instrument would measure atmospheric pressure, and temperature at one sensor location near the camera, high on the lander central body.

In September 1993 a science advisory team (SAT) was appointed to guide the development of the atmosphere structure and meteorology instrument. The advisory team membership consisted of Alvin Seiff (chair), Jeffrey Barnes, David Crisp, Robert Haberle, and James Tillman. This team was appointed by

NASA Headquarters, with the understanding that participation in the operational phase of the mission would be decided by open competition in response to an announcement of opportunity.

During early meetings, the advisory team was concerned that the temperatures measured on the central body were likely to be thermally contaminated by heat from the electronics at the base of the lander center body. This led to a recommendation that a slender meteorology mast be erected after landing, located at the outer end of one of the deployed solar panel petals so as to move the measurements as far as possible from lander heating influences. This mast would also permit temperature measurements at three different heights above the surface to define the near-surface temperature profile in the boundary layer, a new measurement capability not available on Viking. The advisory team also advocated that the measurement set be enlarged to include a simple wind sensor atop the mast, and proposed a concept for the sensor. The SAT assumed responsibility for developing and demonstrating capability of the wind sensor concept. Within limits imposed by safe landing, cost, and complexity, the project accepted the recommendations.

A JPL team was appointed to carry out the detailed design, fabrication, and testing of the instrument. This team was headed by Clayton LaBaw with Colin Mahoney playing a leading technical role.

References

Arvidson, R. E., E. A. Guiness, H. J. Moore, J. E. Tillman, and S. D. Wall, Three Mars years: Viking Lander 1 imaging observations, *Science, 222*, 463–468, 1983.

Baldwin, L. V., V. A. Sandborn, and J. C. Laurence, *ASME Trans. J. Heat Transfer, Ser. C, 82*(2), 77–87, 1960.

Barnes, J. R., Midlatitude disturbances in the Martian atmosphere: A second Mars year, *J. Atmos. Sci., 38*, 225–234, 1981.

Chamberlain, T. E., H. L. Cole, R. G. Dutton, G. C. Greene, and J. E. Tillman, Atmospheric measurements on Mars: The Viking Meteorology Experiment, *Bull. Am. Meteorol. Soc., 57*, 1094, 1976.

Golombek, M. P., R. A. Cook, H. J. Moore, and T. J. Parker, Selection of the Mars Pathfinder landing site, *J. Geophys. Res.*, this issue.

Greeley, R., B. R. White, J. B. Pollack, J. D. Iversen, and R. N. Leach, Dust storms on Mars: Considerations and simulations, *NASA Tech. Memo., TM 78423*, 1977.

Hess, S. L., R. M. Henry, C. B. Leovy, J. A. Ryan, and J. E. Tillman, Meteorological results from the surface of Mars: Viking 1 and 2, *J. Geophys. Res., 82*, 4559–4574, 1977.

Hess, S. L., R. M. Henry, and J. E. Tillman, The seasonal variation of pressure on Mars as affected by the south polar cap, *J. Geophys. Res., 84*, 2923–2927, 1979.

Hess, S. L., J. A. Ryan, J. E. Tillman, R. M. Henry, and C. B. Leovy, The annual cycle of pressure on Mars measured by Viking Landers 1 and 2, *Geophys. Res. Lett., 7*, 197–200, 1980.

James, P. B., and G. R. North, The seasonal cycle of CO$_2$ on Mars: An application of an energy balance climate model, *J. Geophys. Res., 87*, 10,271–10,283, 1982.

Leovy, C. B., Observations of Martian tides over two annual cycles, *J. Atmos. Sci., 38*, 30–39, 1981.

Leovy, C. B., and R. W. Zurek, Thermal tides and Martian dust storms: Direct evidence for coupling, *J. Geophys. Res., 84*(B6), 2956–2968, 1979.

Leovy, C. B., J. E. Tillman, W. R. Guest, and J. Barnes, Interannual variability of Martian weather, recent advances in planetary meteorology, in *Proceedings of Seymour Hess Memorial Symposium*, IUGG Hamburg 1983, edited by Garry Hunt, pp. 69–84, Cambridge Univ. Press, New York, 1985.

Murphy, J. R., C. B. Leovy, and J. E. Tillman, Observations of Martian surface winds at the Viking Lander 1 site, *J. Geophys. Res., 95*(B9), 14,555–14,576, 1990.

Nier, A. O., and M. B. McElroy, Composition and structure of Mars' upper atmosphere: Results from the neutral mass spectrometers on Viking1 and 2, *J. Geophys. Res., 82*(28), 4341-4349, 1977.

OMEGA Engineering, Inc., *Rep OMEGA-91990/1991*, pp. 249-252, Stamford, Conn., 1991.

Paige, D. A., and S. E. Wood, Modeling the Martian seasonal CO_2 cycle, 1, Fitting the Viking Lander pressure curves, Icarus, *99*, 15-27, 1992.

Ryan, J. A., and R. M. Henry, Mars atmospheric phenomena during major dust storms, as measured at the surface, *J. Geophys. Res., 84*, 2821-2829, 1979.

Ryan, J. A., R. M. Henry, S. L. Hess, C. B. Leovy, J. E. Tillman, and C. Waleek, Mars meteorology: Three seasons at the surface, *Geophys. Res. Lett., 5*, 715–718, 1978.

Seiff, A., The Viking atmosphere structure experiment—Techniques, instruments, and expected accuracies, *Space Sci. Instrum., 2*, 381–423, 1976.

Seiff, A., Mars atmospheric winds indicated by motion of the Viking landers during parachute descent, *J. Geophys. Res., 98*(E4), 7461–7474, 1993.

Seiff, A., and D. B. Kirk, Structure of the atmosphere of Mars in summer at mid-latitudes, *J. Geophys. Res., 82*(28), 4364–4378, 1977.

Seiff, A., D. B. Kirk, R. E. Young, R. C. Blanchard, J. T. Findlay, G. M. Kelly, and S. C. Sommer, Measurements of thermal structure and thermal contrasts in the atmosphere of Venus and related dynamical observations: Results from the four Pioneer Venus Probes, *J. Geophys. Res., 85*(A13), 7903–7933, 1980.

Seiff, A., et al., Structure of the atmosphere of Jupiter: Galileo probe measurements, *Science, 272*, 844–845, May 10, 1996.

Smith, P. N. et al., The Imager for Mars Pathfinder experiment, *J. Geophys. Res.*, this issue.

Tillman, J. E., Dynamics of the boundary layer of Mars, in *Proceedings of the Symposium on Planetary Atmospheres*, pp. 145–149, R. Soc. of Can., Ottawa, Ontario, 1977.

Tillman, J. E., Martian meteorology and dust storms from Viking observations, in *Proceedings of the Case for Mars II Conference, Sci. Technol. Ser.*, vol. 62, edited by C. P. McKay, pp. 333–342, Am. Astron. Soc., San Diego, Calif., 1985.

Tillman, J. E., Mars global atmospheric oscillations: Annually synchro-nized, transient normal mode oscillations and the triggering of global dust storms, *J. Geophys. Res., 93*(D8), 9433–9451, 1988.

Tillman, J. E., R. M. Henry, and S. L. Hess, Frontal systems during passage of the Martian north polar hood over the Viking Lander 2 site prior to the first 1977 dust storm, *J. Geophys. Res., 84*, 2947–2955, 1979.

Tillman, J. E., N. C. Johnson, P. Guttorp, and D. B. Percival, The Martian annual atmospheric pressure cycle: Years without great dust storms, *J. Geophys. Res., 98*, 10,963–10,971, 1993.

Wood, S. E., and D. A. Paige, Modeling the Martian seasonal CO_2 cycle, 2, Interannual variability, Icarus, *99*, 1–14, 1992.

Zurek, R. W., Inference of dust opacities for the 1977 Martian great dust storms from Viking Lander 1 pressure data, *Icarus, 45*, 202–215, 1981.

Zurek, R. W., Free and forced modes in the Martian atmosphere, *J. Geophys. Res., 93*, 9452–9462, 1988.

Zurek, R. W., J. R. Barnes, R. M. Haberle, J. B. Pollack, J. E. Tillman, and C. B. Leovy, Mars, in *Dynamics of the Atmosphere of Mars*, chap. 26, pp. 835–933, Univ. of Ariz. Press, Tucson, 1992.

J. R. Barnes, Atmospheric Sciences Department, Oregon State University, Eugene, OR 97331.

D. Crisp, C. LaBaw, C. Mahoney, and J. T. Schofield, MS 169-237, Jet Propulsion Laboratory, NASA, Pasadena, CA 91109.

R. Haberle, J. D. Mihalov, and J. R. Murphy, MS 245-3, Ames Research Center, Moffett Field, CA 94035.

A. Seiff, MS 245-1, Ames Research Center, Moffett Field, CA 94035.

J. E. Tillman, Atmospheric Science Department, University of Washington, MS AK-40, Seattle, WA 98195.

G. R. Wilson, MS 242-6, Ames Research Center, Moffett Field, CA 94035.